1997-01-01

Diffraction from Polarization Holographic Gratings with Surface Relief in Side-chain Azobenzene Polyesters

Izabela Naydenova
Technological University Dublin, izabela.naydenova@tudublin.ie

Ludmila Nikolova
Bulgarian Academy of Sciences

Todor Todorov
Bulgarian Academy of Sciences

See next page for additional authors

Recommended Citation

Naydenova, I. et al. (1998) Diffraction from polarization holographic gratings in side – chain azobenzene polyesters, *J. Opt. Soc. Am. B,* 15, p.1257.

Diffraction from polarization holographic gratings with surface relief in side-chain azobenzene polyesters

I. Naydenova, L. Nikolova, and T. Todorov

Central Laboratory of Optical Storage and Processing of Information, Bulgarian Academy of Sciences, P.O. Box 95, 1113 Sofia, Bulgaria

N. C. R. Holme and P. S. Ramanujam
Optics and Fluid Dynamics Department, Riso. National Laboratory, DK-4000 Roskilde, Denmark

S. Hvilsted
Condensed Matter Physics and Chemistry Department, Riso. National Laboratory, DK-4000 Roskilde, Denmark

Abstract

We investigate the polarization properties of holographic gratings in side-chain azobenzene polyesters in which an anisotropic grating that is due to photoinduced linear and circular birefringence is recorded in the volume of the material and a relief grating appears on the surface. A theoretical model is proposed to explain the experimental results, making it possible to understand the influence of the different photoinduced effects. It is shown that at low intensity the polarization properties of the diffraction at these gratings are determined by the interaction of the linear and circular photobirefringences, and at larger intensity the influence of the surface relief dominates the effect of the circular anisotropy. Owing to the high recording efficiency of the polyesters, the ±1-order diffracted waves change the polarization interference pattern during the holographic recording, resulting in the appearance of a surface relief with doubled frequency.

1. INTRODUCTION

Side-chain azobenzene polymers have been intensively investigated[1–8] in the last decade because of their potential applications in optical storage and holographic optical elements. Their efficiency is due to the large photoinduced linear birefringence (up to 10^{-2}) assigned to the photoinduced orientation of the azobenzene moieties. Photoinduced dichroism in azobenzene-containing systems has been discussed in detail by Rau[9] and Kumar and Neckers.[10] Eich and Wendorff[11] have discussed extensively the application of side-chain liquid-crystalline polymers for three-dimensional holographic storage. The possibility of recording polarization holographic gratings in guest–host systems containing azobenzene was detailed first by Kakichashvili[12] and Todorov *et al.*[13] We have recently developed polyester[14,15] and peptide[16] backbones with pendant azobenzene side chains for erasable holographic storage. The mechanism for optical storage in these materials has been attributed to a statistical reorientation of the azobenzene chromophores perpendicular to the polarization of the incident electric field of the laser beam.[1] The effect of photobleaching by UV light for the erasure of information in side-chain azobenzene polyesters has been outlined by Holme *et al.*[17] In addition to the linear birefringence-induced azobenzene polymers, we have shown that in some side-chain polyesters, circular birefringence is also induced when the exciting light is circularly polarized.[18,19] Earlier, Kakichashvili20 had observed photogyrotropy in mordant azo dyes on irradiation with circularly polarized light. It has also been observed by several groups,[21–23] that, during holographic recording in these polymers, a surface relief grating also appears together with the polarization grating, which is recorded in the volume of the material. The mechanism of the formation of the surface relief is still not clear.

We have investigated the holographic recording in azobenzene polyesters films with two waves that have orthogonal circular polarizations24 and have shown that in this case the relief appears simultaneously with the photoinduced linear anisotropy and that its peaks correspond to the regions where the material is exposed to light polarized along the direction of the grating vector.
The case in which the holographic grating is recorded with two waves with orthogonal linear polarizations turned out to be more interesting. It was observed by atomic force microscopy (AFM)[25] that the relief grating appears with normal frequency (the frequency of the polarization pattern) if the recording waves are polarized at ±45° with respect to the grating vector and with doubled frequency if the recording waves are with vertical (*s*) and horizontal (*p*) polarization.

To elucidate the mechanism of the optical recording in azobenzene polyesters, we investigate here experimentally and theoretically the polarization properties of the diffraction from holographic gratings recorded with two waves with orthogonal linear polarizations by means of both described geometries. In the experiments we have used side-chain azobenzene polyester films in which linear birefringence, circular birefringence, and surface relief are photoinduced. We propose a theoretical model
that explains well all the experimental results obtained and leads to a more complete understanding of the photoprocesses taking place in these materials.

2. EXPERIMENTS

The polyester was prepared by a melt transesterification of diphenyl tetradecanedioate and 2-[6-[4-[4-(cyanophenyl) azo-]phenoxy]-hexyl]-1,3-propanediol under vacuum as previously outlined.[4] This polyester material, denoted P6a12, consists of linear main chains and has weight-average and number-average molecular masses of 43 000 and 17 000, respectively, as determined by sizeexclusion chromatography and use of polystyrene calibration standards. Approximately 22 mg of the polyester
was dissolved in 150 μl of chloroform and spin coated onto clean glass substrates at 1200 rpm. The thickness of the film was measured to be 1.5 μm with a Dektak-3030 surface-profile measuring system.

The geometry of the experiments is shown in Fig. 1. Linearly polarized A^+ laser beams with $\lambda = 488$ nm and equal intensities were used for the recording of the holographic gratings. With the help of two $\lambda/2$ plates their polarizations were set to be at ±45° to the horizontal in one case and at 0° and 90° in the other case. Recording intensities from 70 mW/cm^2 to 750 mW/cm^2 were used. The recording time in all the experiments was 3 min. Since the material retains the recorded gratings after the end of the recording process, we were able to measure the dependence of the diffraction efficiency in the ±1 and ±2 orders on the polarization direction of the reconstructing linearly polarized He–Ne beam. It is verified that the He–Ne beam does not influence the recorded grating. It was established that the intensities of all the diffracted beams in the ±1, ±2, and higher orders are dependent on the input-beam polarization direction. It was also established that these polarization dependencies are different for the two recording geometries used and that they also depend on the recording intensity.

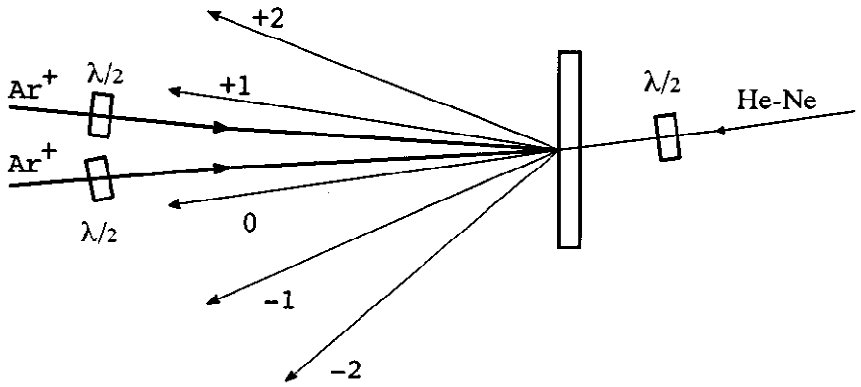

Fig. 1. Geometry of the recording and diffracted beams.

Figure 2 illustrates the experimental results obtained in the case in which the recording beams are polarized at ±45° to the horizontal. The intensity of each diffracted wave was normalized to the sum of the intensities of all the beams behind the film. The curves in Fig. 2(a) correspond to a recording intensity of 100 mW/cm^2 and those in Fig. 2(b) to 750 mW/cm^2. It is seen that the polarization dependence is more pronounced in the ±1 orders and that they are very much different for these two recording intensities. For the lower intensity the maxima and the minima of the curves coincide with the polarization directions of the beams used at the recording (they are marked with arrows in the figure). Furthermore, the intensity of the +1-order beam, I_{+1} , is maximum, where I_{-1} is minimum and vice versa. When a larger recording intensity is used [Fig. 2(b)], the curves $I_{+1}(\alpha)$ and $I_{-1}(\alpha)$ follow each other, and they both have maxima and minima at ±45° with respect to the recording-beam polarizations. At larger recording intensities the polarization dependence is seen to be stronger. We have chosen here curves that fall almost to zero at the minima. At medium recording intensities the maxima and minima are shifted from 0°, 90°, and ±45°, and the curves are not symmetrical; the two maxima do not coincide but they are not shifted to 90°, either.

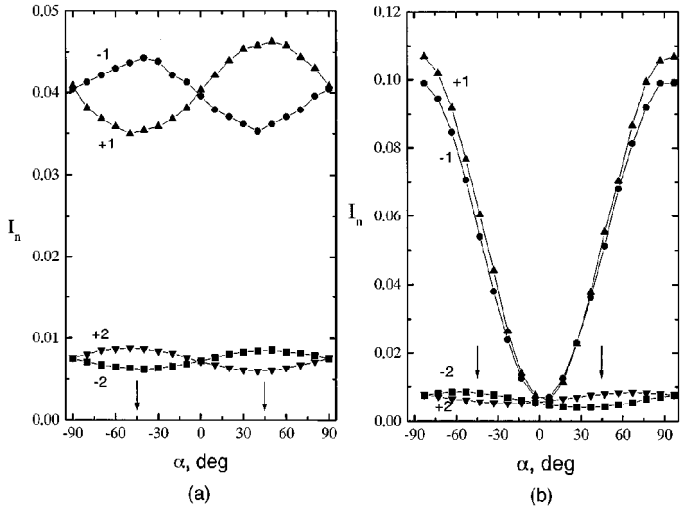

Fig. 2. Experimentally measured dependencies of the normalized intensity I_n (the diffraction efficiency) of the waves diffracted in the +1,-1, +2, and -2 orders on the polarization azimuth α of the reconstructing He–Ne beams. The arrows show the azimuths of the recording beams polarizations: -45° and +45°. The recording intensity is 100 mW/cm^2 [Fig. 2(a)] and 750 mW/cm^2 [Fig. 2(b)].

Figure 3 shows the experimentally observed polarization dependencies $I_{\pm1}(\alpha)$ and $I_{\pm2}(\alpha)$, corresponding to the case in which the two recording beams are polarized at 0° and 90°. We give again a set of curves that illustrate the influence of the recording intensity. At the lower intensity, 150 mW/cm^2 [Fig. 3(a)], the curves $I_{\pm1}(\alpha)$ and $I_{\pm2}(\alpha)$ are very much like those in Fig. 2(a), only the maxima and minima are shifted; they coincide again with the recording beams' polarization azimuths. The values of the two maxima are not equal, and the ratio I_{max}/I_{min} for the ±2 orders is higher than that in the case shown in Fig. 2(a). For the larger recording intensity, 600 mW/cm^2 [Fig. 3(b)], the picture is different. The intensities I_{+1} and I_{-1} are almost independent of the input polarization. The dependence of I_{+2} on α is very strong, but I_{-2} is almost constant. In some experiments made at still higher intensity, the minimum and maximum of the curve $I_{+2}(\alpha)$ interchange; that is, the two curves have maxima simultaneously.

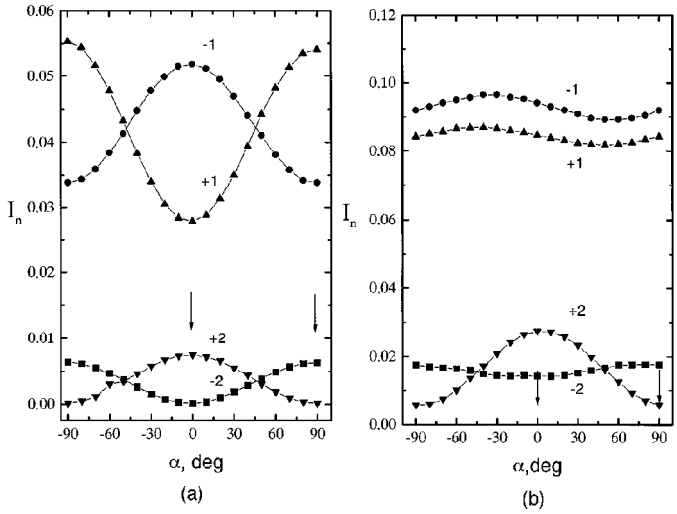

Fig. 3. Experimentally measured curves $I\pm1(\alpha)$ and $I\pm2(\alpha)$ in the case in which the recording waves are with horizontal (0°) and vertical (90°) polarizations. The recording intensity is 150 mW/cm^2 [Fig. 3(a)] and 600 mW/cm^2 [Fig. 3(b)].

It is evident from these results that different processes are taking place or predominate at different recording intensities, and it is also seen that these processes differ for the two recording geometries. As was already mentioned, it is known from AFM investigations[25] that in the case of recording beams polarized at ±45° a relief grating with normal frequency appears, and when the recording beams are at 0° and 90°, a relief with doubled frequency is observed. It is not possible, however, from AFM only, to locate the peaks of these relief gratings with respect to the recording polarization pattern. To better understand these photoinduced processes, we made a theoretical analysis of the diffraction from polarization holographic gratings in materials in which all three effects are observed: linear birefringence, circular birefringence, and photoinduced surface relief.

3. THEORY

It is known that the interference pattern of two coherent waves with orthogonal linear polarizations has a constant intensity and a polarization state that is periodically modulated. When the two interfering waves have equal intensities, the light polarization changes from linear to circular, orthogonal linear, orthogonal circular, and so on; the directions of the linear polarizations are at ±45° with respect to the polarization directions of the recording waves (Fig. 4). Thus if the recording waves are polarized at ±45° with respect

to the horizontal, the interference field appears as shown in Fig. 4(a), and if they are vertically and horizontally polarized, the interference field appears as in Fig. 4(b).

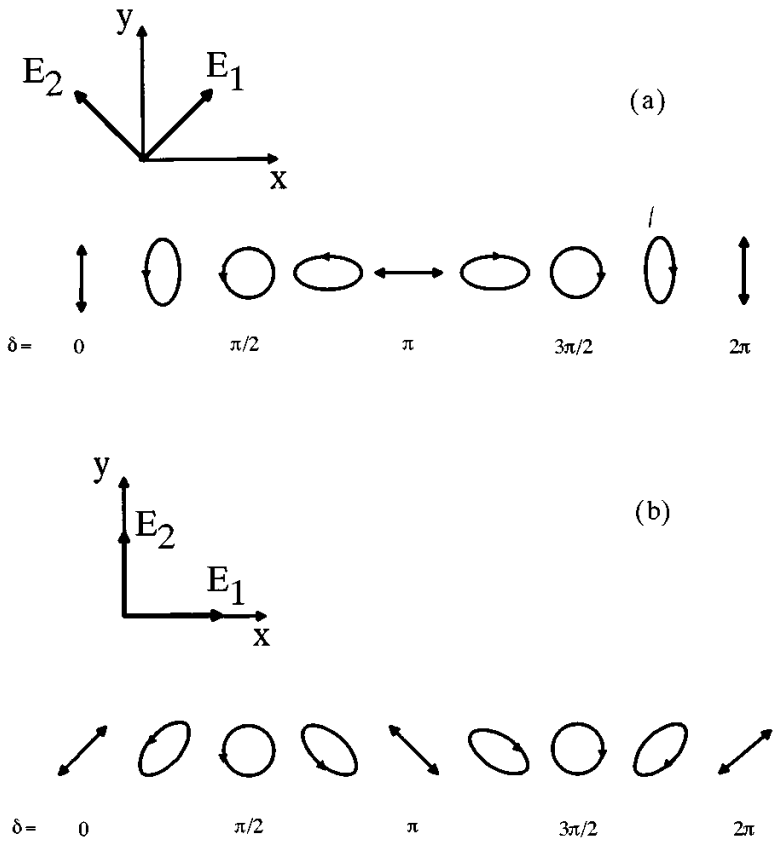

Fig. 4. Polarization modulation of the interference light field recording the gratings in the two geometries used, (a) and (b). E_1 and E_2 are the polarization vectors of the two recording waves, and δ is the phase difference between them.

In the side-chain azobenzene polyester this interference field induces linear anisotropy in the regions with linear polarization and circular anisotropy in the regions with circular polarization. The elliptic polarization induces both linear and circular anisotropy. So the material becomes anisotropic; its anisotropy is periodically modulated in accordance with the polarization state of the recording light field. We assume here that a phase grating is recorded; that is, the photoinduced changes are only in the refractive index n of the material. This assumption is valid for λ= 633 nm because the polyester films have practically no absorption at this wavelength. At 488 nm the absorption is significant, and polarized light induces anisotropy in the optical density (dichroism) in addition to the photoinduced birefringence. However, since the maximum induced dichroism is approximately 0.15 and the photobirefringence is as large as 0.01, we consider here as negligible the amplitude part of the polarization grating. As it has been shown in Ref. 19, the photoinduced anisotropic changes in the refractive index (Δn) are described by

$$\Delta \mathbf{n} = \begin{vmatrix} k_s S_0 + k_{\text{lin}} S_1 & k_{\text{lin}} S_2 + i k_{\text{cir}} S_3 \\ k_{\text{lin}} S_2 - i k_{\text{cir}} S_3 & k_s S_0 - k_{\text{lin}} S \end{vmatrix}, \qquad (1)$$

where S_0 , S_1 , S_2 , and S_3 are the four Stokes parameters of the recording light field, k_s is a coefficient of the scalar photoresponse of the material, and k_{lin} and k_{cir} are the coefficients of the linear and circular photoanisotropy. For the two recording geometries that we used we have

$$\begin{aligned} S_0 &= I = \text{const.}, \\ S_1 &= I \cos \delta, \\ S_2 &= 0, \\ S_3 &= -I \sin \delta, \end{aligned} \qquad (2)$$

when the recording waves polarization are at ±45°, and

$$\begin{aligned} S_0 &= I = \text{const.}, \\ S_1 &= 0, \\ S_2 &= I \cos \delta, \\ S_3 &= -I \sin \delta, \end{aligned} \qquad (3)$$

when the recording waves are polarized along the horizontal and the vertical. Here I is the recording intensity and δ is the phase shift between the recording waves. Because the parameter S_0 (the intensity) is not modulated at the polarization recording, the term $k_s S_0$ gives a nonmodulated change in the refractive index that does not influence the diffraction at the grating. Moreover, we know from previous experiments that the scalar photoresponse in our material is negligible with respect to the photoinduced anisotropy, so that further in this analysis we have put $k_s S_0 = 0$.

The Jones matrix that describes the phase transmittance of the recorded anisotropic grating and the diffraction from it can be obtained as:

$$\begin{aligned} T_{\text{an}} &= \exp[i(2\pi/\lambda)(n_0 + \Delta \mathbf{n})d] \\ &= \exp(i\varphi_0)\exp[i(2\pi/\lambda)\Delta \mathbf{n} d], \end{aligned} \qquad (4)$$

where n_0 is the refractive index of the material before the holographic recording, d is the film thickness, λ is the wavelength, and $\varphi_0=(2\pi/\lambda)n_0 d$. To analyze the anisotropic diffraction from this grating one must multiply the Jones vector of the wave incident on it (E_{in}) by the matrix T_{an} :

$$E_{\text{out}} = T_{\text{an}} E_{\text{in}} . \qquad (5)$$

When a surface relief grating is also formed during the holographic recording, light is diffracted from this grating, too, so finally the diffracted field is determined by:

$$E_{\text{out}} = R T_{\text{an}} E_{\text{in}} = T_{\text{tot}} E_{\text{in}} . \qquad (6)$$

The matrix R that describes the diffraction at the relief grating can be written as:

$$R = \begin{bmatrix} \exp(i\Delta\psi) & 0 \\ 0 & \exp(i\Delta\psi) \end{bmatrix}, \qquad (7)$$

where

$$\Delta\psi = (2\pi/\lambda) r_1 [(n_p - n_a)/2] \cos(\delta + \Delta_1), \qquad (8)$$

when the relief grating has the same frequency as the polarization grating and

$$\Delta\psi = (2\pi/\lambda) r_2 [(n_p - n_a)/2] \cos 2(\delta + \Delta_2), \qquad (9)$$

when the relief is with doubled frequency. Here n_p and n_a are the refractive indices of the polymer and the air, and Δ_1 and Δ_2 are phase constants that account for the spatial shift of the relief with respect to the recording polarization pattern. r_1 is the height of the surface modulation at the fundamental frequency and r_2 , that of the doubled frequency. The fundamental frequency is here defined to be the frequency of the polarization grating.

The expression that is obtained for E_{out} contains all the information about the waves diffracted in the different orders, their intensities, and their polarizations. The problem in this approach arises from the rather intricate form of the elements of the matrix T_{tot} in the general case. It is due, first of all, to the simultaneous inducement of both linear and circular birefringence in the material. Diffraction from polarization holographic gratings in azobenzene polyesters with linear and circular photoanisotropy was investigated in Ref. 18. It was shown that simple expressions can be obtained only if small photoinduced changes are assumed. This approximation limits the consideration to the diffraction in the ±1 orders only. No analytical expressions can be derived in the general case to describe the diffraction in the higher orders. Things are even more complicated when a surface relief grating must be included in the calculations.

There is one more effect that has to be taken into account. In highly efficient real-time holographic materials, very soon after the beginning of the recording at least four diffracted waves appear in addition to the two recording waves: two +1-order waves and two -1-order waves. If their intensity is high enough (as it is in azobenzene polyesters) these diffracted waves influence the further recording process.[26] In the case of polarization recording they change the polarization pattern that record the grating, and finally the shape of the modulation of the anisotropic changes in the refractive index.

To be able to take into account all these interacting effects, we wrote a computer program to (1) calculate the elements of the matrix T_{tot} as functions of the intensity and the polarization of the recording waves, the coefficients k_{lin} and k_{cir} , the intensity I, the height of the relief r_1 or r_2 , their phase shifts Δ_1 or Δ_2 , and the index n_p , (2) calculate the components of the output field E_{out}; (3) perform the Fourier analysis of these components, and (4) find the intensities and the polarizations of the waves diffracted in the ±1, ±2, and higher orders as functions of the polarization of the wave incident on the grating. The program allows the calculation to be made with and without taking into account the influence of the ±1-order diffracted waves during the recording. When these waves are included in the formation of the recording polarization pattern, their amplitudes are taken to be equal to the values of the first-order Bessel function of first kind corresponding to the photoinduced anisotropic modulation of the refractive index obtained with the two recording waves only, and their polarizations are taken to be orthogonal to the corresponding zeroth-order wave. This approach is approximate, but it gives results that make it possible for us to explain the polarization dependencies obtained experimentally and to understand how to separate the influence of the different photoinduced effects and how to determine which of them is dominating.

Here we give some typical curves illustrating the calculated dependencies of the intensities of the waves diffracted in the ±1 and ±2 orders on the polarization azimuth of the input wave for the different cases in which linear and circular birefringences are induced, and surface relief with normal or doubled frequency also appears during the holographic recording.

The curves in Fig. 5 are calculated without taking into account the influence of the diffracted waves during the recording. For Figs. 5(a)–5(c) the two recording waves are taken to be polarized at ±45°, and the grating vector is along 0°. Figure 5(a) illustrates the diffraction from the anisotropic grating only ($T_{tot} = T_{an}$), that is, with $k_{lin} \neq 0$, $k_{cir} \neq 0$, $r_1 = 0$, and $r_2 = 0$. It is seen that only the intensities I_{+1} and I_{-1} are polarization dependent. The positions of their maxima coincide with the polarization direction of the recording beams. The analysis shows that the amplitudes of these curves depend on the ratio k_{cir}/k_{lin} : the larger this ratio is, the larger the amplitudes are. The next figure [Fig. 5(b)] shows the curves $I\pm1(\alpha)$ and $I\pm2(\alpha)$ calculated with $k_{lin}\neq0$, $k_{cir} = 0$, $r_1 \neq 0$, $\Delta_1 = \pi$, and $r_2 = 0$ (only linear birefringence and surface relief with normal frequency are photoinduced, and the peaks of the relief are in the regions exposed to horizontally polarized light). In this case all four diffracted intensities depend on the input polarization. The positions of all the maxima coincide, and they all are shifted at 45° with respect to the recording waves' polarizations. The zeroth-order intensity is also polarization dependent in this case. If Δ_1 is taken to be 0°, the maxima and minima of all the curves interchange. No polarization dependence is obtained with $\Delta_1 = \pi/2$ or $3\pi/2$. Figure 5(c) shows the same curves but with $k_{cir} \neq 0$; circular birefringence is also photoinduced. It influences the positions of the maxima in the curves $I_{+1}(\alpha)$ and $I_{-1}(\alpha)$. The curves in Figs. 5(d) and 5(e) are calculated assuming that a relief grating with doubled frequency appears at the recording, and it is shifted by $\pi/4$ with respect to the polarization pattern. The polarizations of the recording waves are taken to be at 0° and 90°. Figure 5(d) corresponds to the case in which no circular birefringence is induced: $k_{lin} \neq 0$, $k_{cir} = 0$, $r_1 = 0$, $r_2 \neq 0$, and $\Delta_2 = \pi/4$. There is no polarization dependence of any of the diffracted intensities but $I_{+1} < I_{-1}$ and $I_{+2} > I_{-2}$. If $\Delta_2=3\pi/4$, we obtain $I_{+1} > I_{-1}$ and $I_{+2} < I_{-2}$, and if $\Delta_2 = 0$, $\pi/2$, or π, then $I_{+1}=I_{-1}$ and $I_{+2} = I_{-2}$. Figure 5(e) shows the same curves in the case in which circular birefringence is also induced; it results in polarization dependent I_{+1} and I_{-1}, and their mean values remain different. The zeroth-order intensity is also polarization dependent. It can be seen that the theoretical curves $I_{+1}(\alpha)$ and $I_{-1}(\alpha)$ in Fig. 5(a) look like the corresponding experimental curves in Fig. 2(a) and Fig. 3(a) [the coordinate system must be rotated to 45° for the curves in Fig. 3(a)]. The calculated curves for I_{+2} and I_{-2} , however, do not explain the dependencies $I_{\pm2}(\alpha)$. The ±1-order curves in Fig. 5(b) resemble the corresponding curves in Fig. 2(b). The second-order curves in these figures are not coinciding well again. And finally, the curves in Fig. 3(b) cannot be explained with any of the theoretical examples. We believe that the reason for this noncoincidence is that the influence of the diffracted waves on the real-time holographic recording is not involved in these calculations. Our analysis has shown that

to describe satisfactorily the experimental results with this theoretical model, it is sufficient to take into account the waves diffracted in the ±1 orders. The curves in the next figures are calculated in this way, and they explain much better the experimentally measured dependencies.

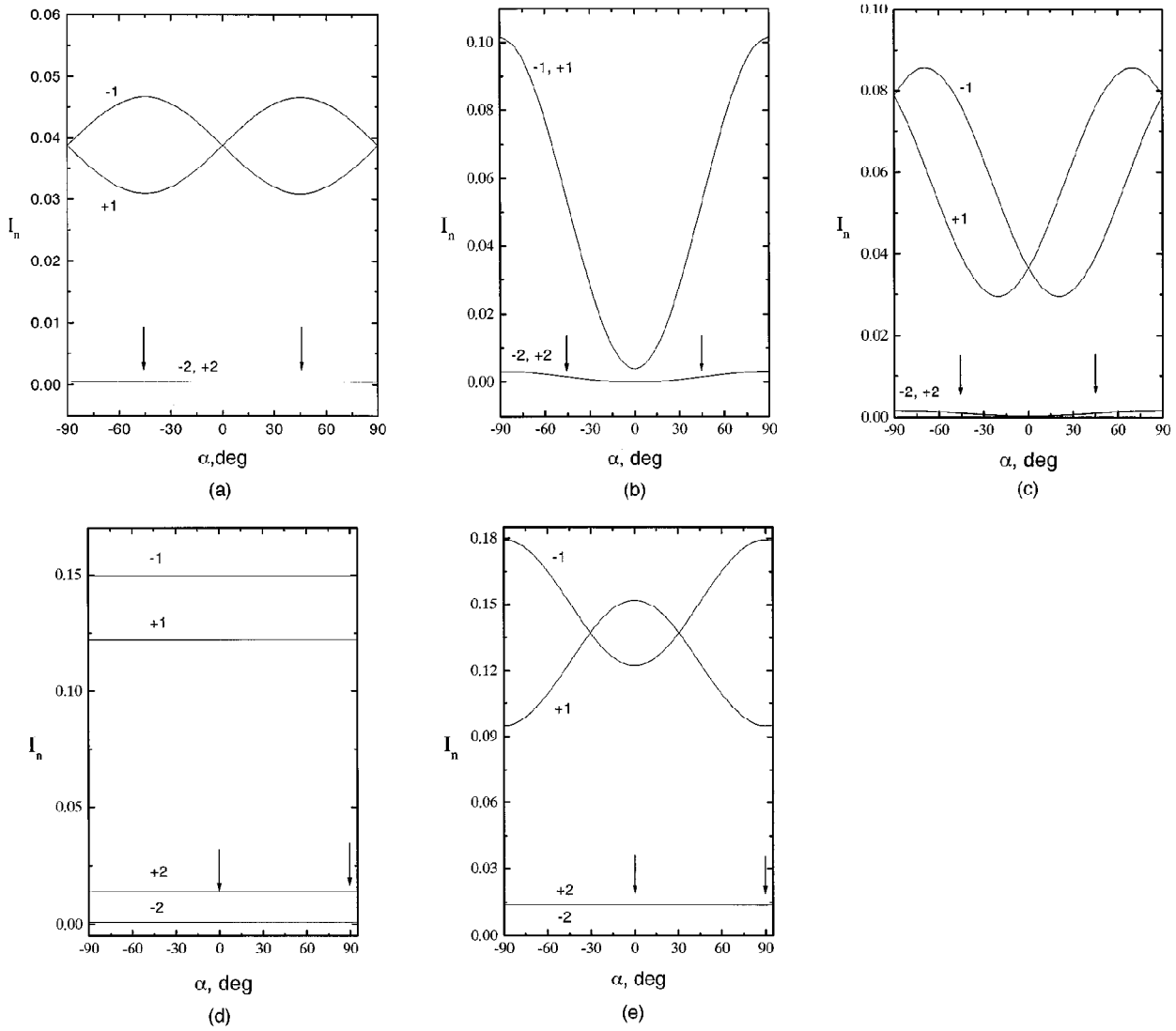

Fig. 5. Theoretical curves for $I_{\pm1}(\alpha)$ and $I_{\pm2}(\alpha)$. The first row of figures corresponds to recording waves polarized at ±45°; the second row corresponds to recording waves at 0° and 90°. (a): $\Delta\varphi_{lin} = (2\pi/\lambda)k_{lin}\, Id$ = -0.39; $\Delta\varphi_{cir} = (2\pi/\lambda)k_{cir}\, Id$ = -0.048; $r_1 = 0$, $r_2 = 0$; (b): $\Delta\varphi_{lin}$ = -0.45, $\Delta\varphi_{cir} = 0$, r_1 = 200 nm, $\Delta_1 = \pi$; (c): $\Delta\varphi_{lin}$ = -0.45, $\Delta\varphi_{cir}$ = -0.05, r_1 = 200 nm, $\Delta_1 = \pi$; (d): $\Delta\varphi_{lin}$ = -0.4, $\Delta\varphi_{cir} = 0$, $r_1 = 0$, r_2 = 80 nm, $\Delta_2 = \pi/4$; (e): $\Delta\varphi_{lin}$ = -0.4, $\Delta\varphi_{cir}$ = 0.05, r_1= 0, r_2 = 80 nm, $\Delta_2 = \pi/4$. The effect of the diffracted waves on the recording interference field is not taken into account in these calculations.

The curves in Fig. 6(a) are calculated with $r_1 = 0$, $r_2 = 0$, and by taking for the amplitudes of the anisotropic phase modulations that are due to the linear photobirefringence $\Delta\varphi_{lin} = (2\pi/\lambda)k_{lin}\, Id$ and to the circular photobirefringence $\Delta\varphi_{cir} = (2\pi/\lambda)k_{cir}\, Id$, the values are $\Delta\varphi_{lin}$ = -0.4 and $\Delta\varphi_{cir}$ = -0.05, respectively. They are very much like the curves in Fig. 2(a), including the curves for $I_{\pm2}(\alpha)$, and to a certain degree the curves in Fig. 3(a) (shifted to 45° as the recording-beam polarizations are shifted to 45° for these curves). That is, to explain the experimental curves in Figs. 2(a) and 3(a), one must suppose that

at low intensity the phase modulation that is due to surface relief is negligible, and the polarization dependencies of $I_{\pm1}$ and $I_{\pm2}$ are due almost entirely to the interaction of the linear and circular birefringences.

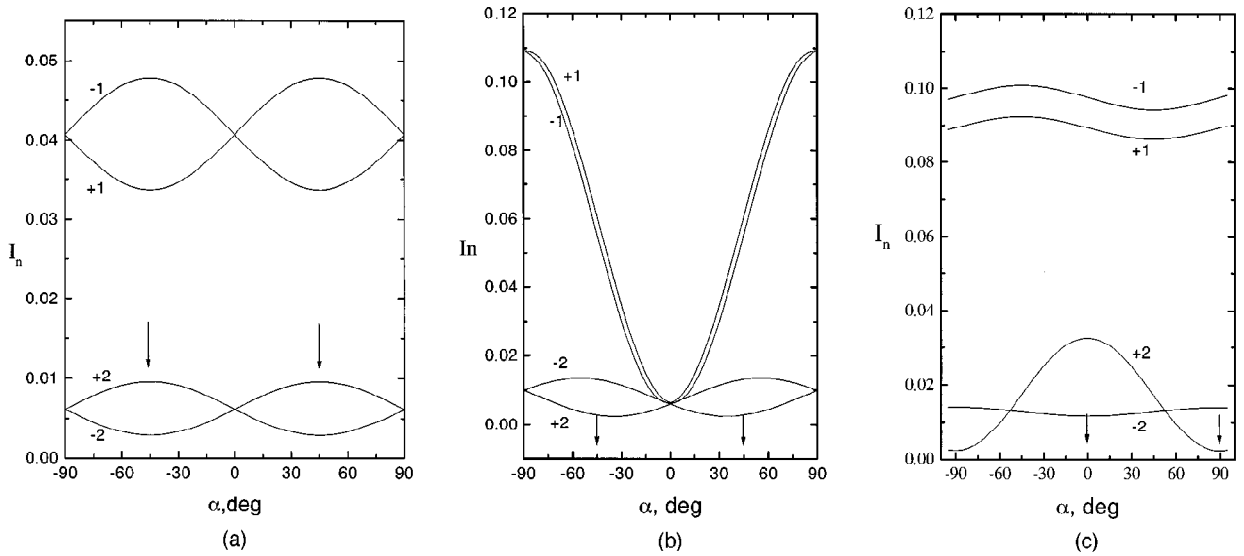

Fig. 6. Theoretical curves for $I_{\pm1}(\alpha)$ and $I_{\pm2}(\alpha)$ calculated in the case in which the influence of the ±1-order diffracted waves on the polarization modulation of the recording light field is taken into account. (a): $\Delta\varphi_{lin} = -0.39$, $\Delta\varphi_{cir} = -0.048$, $r_1 = 0$, $r_2 = 0$; (b): $\Delta\varphi_{lin} = -0.5$, $\Delta\varphi_{cir} = 0$, $r_1 = 440$ nm, $\Delta_1 = \pi$, $r_2 = 0$; (c): $\Delta\varphi_{lin} = -0.5$, $\Delta\varphi_{cir} = 0$, $r_1 = 10$ nm, $\Delta_1 = \pi$, $r_2 = 90$ nm, $\Delta_2 = \pi/4$.

The curves in Fig. 6(b) are calculated with $\Delta\varphi_{lin} = -0.5$, $\Delta\varphi_{cir} = 0$, $r_1 = 440$ nm, $\Delta_1 = \pi$, and $r_2 = 0$. Their resemblance to the experimental curves in Fig. 2(b) is obvious. Thus one can explain the curves in Fig. 2(b) by assuming that there is no photoinduced circular birefringence in this case, and a relief grating with normal frequency is induced only in addition to the photoinduced periodically modulated linear birefringence. This coincides with the observation by AFM of a relief with normal frequency. To fit the theory to the experiment, this relief grating must be assumed to have shifted to p with respect to the interference pattern; the peaks of the relief are in the regions exposed to horizontally polarized light [see Fig. 4(a)].

The last set of curves, shown in Fig. 6(c) is calculated with $\Delta\varphi_{lin} = -0.05$, $\Delta\varphi_{cir} = 0$, $r_1 = 10$ nm, $\Delta_1 = \pi$, $r_2 = 90$ nm, and $\Delta_2 = \pi/4$. The recording waves are taken to be at 0° and 90°. The curves $I_{+2}(\alpha)$ and $I_{-2}(\alpha)$ resemble very much the experimental curves for I_{+2} and I_{-2} in Fig. 3(b). The same unusual asymmetry is obtained. It is due to the presence of a relief grating with doubled frequency shifted to $\pi/4$ with respect to the anisotropic grating. No circular birefringence is assumed at these calculations. For the maxima in the curves $I_{+1}(\alpha)$ and $I_{-1}(\alpha)$ to coincide and to be shifted at 45° with respect to the polarization directions of the recording waves, a very weak first-order relief grating is also assumed; if $r_1 = 0$, the values of I_{+1} and I_{-1} are constant, and $I_{+1} < I_{-1}$.

4. DISCUSSION

It can be concluded from the results presented here that our theoretical model satisfactorily explains the unusual dependencies of the intensities of the diffracted waves on the polarization direction of the input wave. Therefore one can use it to analyze the photoprocesses that take place in the films during the holographic recording while keeping in mind the corresponding experimental results. We think that there are two important results from these investigations concerning the photoprocesses in the azobenzene

polyesters. The first of them is the fact that circular birefringence is induced in these films only at lower-intensity holographic recording. At higher intensities the surface relief is much more important, and it seems that there is practically no more circular anisotropy. In the case in which the two recording waves are polarized along ±45° the surface relief is at normal frequency (the frequency of the anisotropic grating in the volume of the material), and its peaks are located in the regions illuminated with horizontal polarization (along the grating vector).

The second important result is related to the appearance of the relief grating with doubled frequency. To begin with, it is not at all evident why the relief appears with doubled frequency in the case in which the recording waves are polarized at 0° and 90°. Furthermore, by fitting the theoretical curves to the experimental ones in Fig. 3(b), we find that the double-frequency relief is shifted by $\pi/4$ with respect to the interference pattern. This means that its peaks do not coincide with the places exposed to linearly or circularly polarized light; they are in regions exposed to elliptic polarization. We can explain this result only with the influence of the ±1-order diffracted waves on the formation of the final diffraction grating. When these waves are included in the formation of the interference light field that record the grating, this interference field is no longer that shown in Fig. 4(b). The polarization pattern changes, and the Stokes parameters of the recording light are no longer described by Eq. (3), but by more complicate functions. An example is given in Fig. 7. The curves for S_1 , S_2 , and S_3 in this figure correspond to the case shown in Fig. 6(c). It is seen at once that the parameter S_1 , which equals the difference of the intensities of the horizontal and vertical components of the light field and which is zero in the beginning of the recording [see Eq. (3)], is no longer zero or a constant. It is a periodic function of the phase difference δ between the two recording waves, and this periodic function is with a doubled frequency. Its maxima, the places where the horizontal component of light is the most intensive, are at $\delta = 3\pi/4$ and $\delta = 7\pi/4$; that is, we can describe S_1 approximately with $S_1 \propto \cos[2(\delta + \pi/4)]$. We conclude therefore that the relief with doubled frequency follows the modulation of the parameter S_1 , and its peaks appear in the places where the intensity of the horizontal component is maximum.

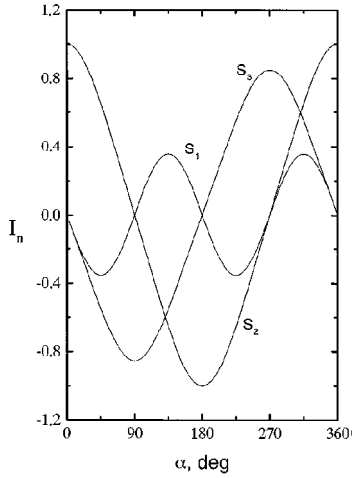

Fig. 7. Modulation of the Stokes parameters S_1 , S_2 , and S_3 when the influence of the waves diffracted in the ±1 orders on the polarization pattern is taken into account.

To verify this assumption, we have recorded three gratings on the same material and with the same recording geometry, with two waves polarized at 0° and 90°, using different exposure times of 5 s, 10 s, and 20 s. The images of the AFM scan of the surfaces of these gratings are shown in Fig. 8. The frequency of the surface relief of the grating obtained with short exposure time (5 s) corresponds to the frequency of the polarization interference pattern; the relief changes its shape when the exposure time is increased (10 s), and the frequency is doubled for the grating corresponding to an exposure time of 20 s.

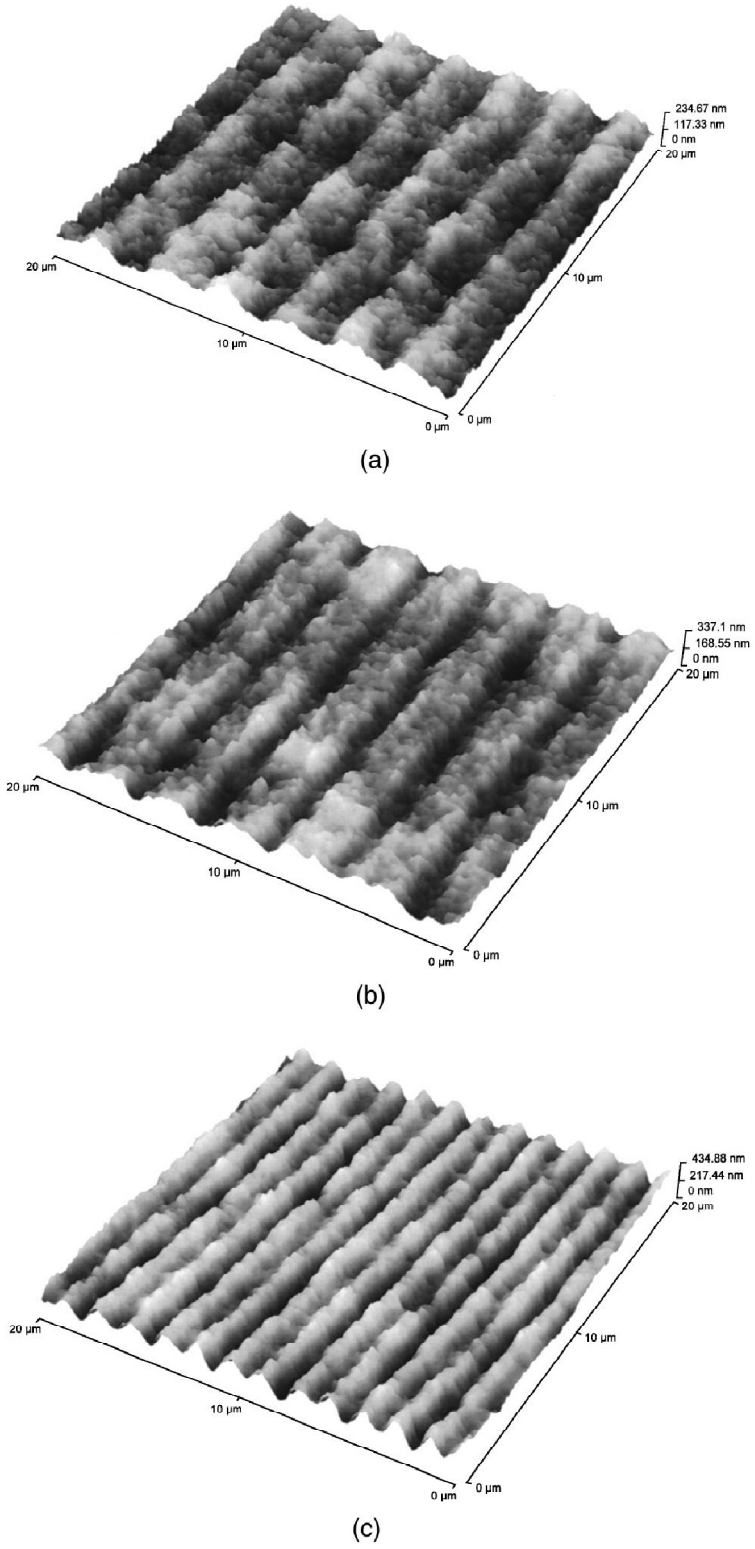

Fig. 8. AFM scan of the surface of holographic gratings recorded with two waves linearly polarized at 0° and 90°, λ = 488 nm, I = 750 mW/cm^2 and exposure time (a) 5 s, (b) 10 s, and (c) 20 s.

We believe that the appearance of the weak relief with normal frequency [Fig. 8(a)] is due to some small asymmetry I_n the geometry of the recording. The analysis shows that if the polarizations of the recording waves are not exactly parallel and orthogonal to the grating vector, the parameter S_1 is not constant even at the beginning of the recording, when only two waves are forming the polarization pattern. It is a periodic function with the normal period, and its amplitude is not negligible even for errors of a few degrees in the polarization angles. When the ±1-order diffracted waves appear, they change the shape of the modulation of S_1 , and the shape of the relief also changes. Finally S_1 changes to the doubled frequency (see Fig. 7), as does the surface relief [Fig. 8(c)]. The fact that the peaks of the relief are at the places where S_1 has its maxima coincides with the results of our investigation of the relief's appearing at the holographic recording with two waves with orthogonal circular polarizations [24] (the peaks correspond to the horizontal polarization in the interference recording field) as well as with the results in the case of recording with two waves polarized at ±45° (the peaks in this case are obtained again in the regions where S_1 has its maxima). In the latter case the waves diffracted in the ±1 orders do not change the frequency of the modulation of S_1 but only change its shape; it is no longer sinusoidal, but the places of the maxima remain unchanged so that the photoinduced relief is of normal frequency. In this case (with recording waves at ±45°) the parameter S_2 that is initially zero becomes a periodic function with doubled frequency during the holographic recording, but obviously the difference between the intensities of the components polarized along +45° and -45° does not influence the formation of the surface relief. This confirms once more our conclusion that the relief grating in the material investigated here is determined by the modulation of the horizontal component of the interference recording field. The exact mechanism of the formation of the surface relief is not clear to us at this time, but we believe that more detailed experiments comparing the properties of holographic gratings recorded in different types of azobenzene polymers would result in better understanding of this process.

ACKNOWLEDGMENTS

This work was funded by the National Science Fund of Bulgaria under contract F-440 and the Danish Research Academy through the award of a doctoral stipend to C. Holme and a guest professorship to L. Nikolova. This project was also supported by the Danish Materials Technology Development program (MUP 2). We also thank DanDisc A/S, Denmark, for their kind loan of the Dektak surface-profile measuring instrument.

REFERENCES

1. M. Eich, J. H. Wendorff, B. Reck, and H. Ringsdorf, ''Reversible digital and holographic optical storage in polymeric liquid crystals,'' Makromol. Chem. Rapid Commun. **8**, 59–63 (1987).
2. U. Wiesner, M. Antonietti, C. Boeffel, and H. W. Spiess, ''Dynamics of photoinduced isomerization of azobenzene moieties in liquid-crystalline polymers,'' Makromol. Chem. **191**, 2133–2149 (1990).
3. V. P. Shibaev, I. V. Yakolev, S. G. Kostromin, S. A. Invanov, and T. I. Sverkova, ''Specific features of optical information storage in oriented films of liquid crystalline comb-like polymers by means of selective optical excitation,'' Vysokomol. Soyed. A **32**, 1552–1559 (1990).
1264 J. Opt. Soc. Am. B/ Vol. 15, No. 4/ April 1998 Naydenova *et al.* 4. A. Natansohn, P. Rochon, J. Gosselin, and S. Xie, ''Azo polymers for reversible optical storage. 1. Poly[48 - [[2- (acryloyoxy) ethyl]ethylamino] - 2 - chloro - 4 - nitroazoben - zene],'' Macromolecules **25**, 2268–2273 (1992).
5. Th. Fischer, L. La¨sker, J. Stumpe, and S. G. Kostromin, ''Photoinduced optical anisotropy in films of photochromic liquid crystalline polymers,'' J. Photochem. Photobiol. A **80**, 453–459 (1994).
6. H. H. Haitjema, G. L. von Morgen, Y. Y. Tan, and G. Challa, ''Photoresponsive behavior of azobenzene-based (meth)acrylic (co)polymers in thin films,'' Macromolecules **27**, 6201–6206 (1994).
7. Z. Sekkat, M. Bu¨ chel, H. Orendi, H. Menzel, and W. Knoll, ''Photoinduced alignment of azobenzene moieties in the side chains of polyglutamate films,'' Chem. Phys. Lett. **220**, 497–501 (1994).
8. M. Scho¨nhoff, L. F. Chi, H. Fuchs, and M. Lo¨sche, ''Structural rearrangements upon photoorientation of amphiphilic azobenzene dyes organized in ultrathin films on solid surfaces,'' Langmuir **11**, 163–168 (1995).
9. H. Rau, ''Spektroskopische eigenschaften organischer Azoverbindungen,'' Angew. Chem. **85**, 248–258 (1973).
10. G. S. Kumar and D. C. Neckers, ''Photochemistry of azobenzene containing polymers,'' Chem. Rev. **89**, 1915–1925 (1989).

11. M. Eich and J. H. Wendorff, ‘‘Laser-induced gratings and spectroscopy in monodomains of liquid-crystalline polymers,’’ J. Opt. Soc. Am. B **7**, 1428–1436 (1990).
12. Sh. D. Kakichashvili, ‘‘Polarization recording of holograms,’’ Opt. Spectrosc. **33**, 171–173 (1972).
13. T. Todorov, L. Nikolova, and N. Tomova, ‘‘Polarization holography. 1: A new high-efficiency organic material with reversible photoinduced birefringence,’’ Appl. Opt. **23**, 4309–4312 (1984).
14. S. Hvilsted, F. Andruzzi, and P. S. Ramanujam, ‘‘Side-chain liquid crystalline polyesters for optical information storage,’’ Opt. Lett. **17**, 1234–1236 (1992).
15. S. Hvilsted, F. Andruzzi, C. Kulinna, H. W. Siesler, and P. S. Ramanujam, ‘‘Novel side-chain liquid-crystalline polyesters architecture for reversible optical storage,’’ Macromolecules **28**, 2172–2183 (1995).
16. R. H. Berg, S. Hvilsted, and P. S. Ramanujam, ‘‘Peptide oligomers for holographic storage,’’ Nature (London) **383**, 505–509 (1996).
17. N. C. R. Holme, P. S. Ramanujam, and S. Hvilsted, ‘‘10 000 optical write, read, and erase cycles in an azobenzene sidechain liquid-crystalline polyester,’’ Opt. Lett. **21**, 902– 904 (1996).
18. L. Nikolova, T. Todorov, M. Ivanov, F. Andruzzi, S. Hvilsted, and P. S. Ramanujam, ‘‘Polarization holographic grating in side-chain azobenzene polyesters with linear and circular photoanisotropy,’’ Appl. Opt. **35**, 3835–3840 (1996).
19. I. Naydenova, L. Nikolova, T. Todorov, F. Andruzzi, S. Hvilsted, and P. S. Ramanujam, ‘‘Polarimetric investigation of materials with both linear and circular anisotropy,’’ J. Mod. Opt. **44**, 1643–1650 (1997).
20. Sh. D. Kakichashvili, ‘‘Gyrotropy (photogyrotropy) induced in mordant azo dyes by induced circularly polarized light,’’ Sov. Tech. Phys. Lett. **16**, 736–737 (1990).
21. P. Rochon, E. Batalla, and A. Natansohn, ‘‘Optically induced surface gratings on azoaromatic polymer films,’’ Appl. Phys. Lett. **66**, 136–138 (1995).
22. D. Y. Kim, S. K. Tripathy, L. Li, and J. Kumar, ‘‘Laser induced holographic surface relief gratings on nonlinear optical polymer films,’’ Appl. Phys. Lett. **66**, 1166–1168 (1995).
23. P. S. Ramanujam, N. C. R. Holme, and S. Hvilsted, ‘‘Atomic force and optical near-field microscopic investigation of polarization holographic gratings in a liquid crystalline azobenzene side-chain polyester,’’ Appl. Phys. Lett. **68**, 1329–1331 (1996).
24. N. C. R. Holme, L. Nikolova, P. S. Ramanujam, and S. Hvilsted, ‘‘An analysis of the anisotropic and topographic gratings in a side chain liquid-crystalline azobenzene polyester,’’ Appl. Phys. Lett. **70**, 1518–1521 (1997).
25. N. C. R. Holme, ‘‘Photoinduced anisotropy, holographic gratings and near-field optical microscopy in side-chain azobenzene polyesters,’’ Ph.D. dissertation, Riso. Rep. R-983(EN) (Riso. National Laboratory, Roskilde, Denmark, 1997).
26. T. Huang and K. H. Wagner, ‘‘Holographic diffraction in photoanisotropic organic materials,’’ J. Opt. Soc. Am. A **10**, 306–315 (1993).